ECC '88

A TECHNIQUE FOR ELECTRICAL MEASUREMENT OF BALL BOND LOCATION

C. G. Shirley and S. Gupta
Intel Corporation
Component Assembly/Test
145 S. 79th St.
Chandler, AZ 85226

Abstract

A test structure incorporating a special bond pad can be used to make an electrical measurement of the location of a ball bond on a bonding pad. The pad can also be used to measure the electrical resistance of a wire and its bond interfaces (Kelvin measurement). The structure consists of an aluminum bond pad with each corner connected to another bond pad. Four of these 5-pad sense elements are incorporated into small square test die "modules". For any specific application test dice can be cut from the wafer in multiples of the module. We describe the method and theory of location measurement, and present data to verify the operation of the sensors.

Introduction

Ball-bond misplacement is a potential source of assembly yield loss and of reliability concerns. Many sources of error can contribute to the misplacement of a bond: for example, wear can degrade mechanical tolerances in the bonding tool or package support fixtures etc. Meaningful evaluation of the yield impact of bond misplacement will involve a study of the distribution of bond locations over a large number of samples produced under production conditions. Unfortunately, conventional methods for gathering data on bond location for a large sample size are either tedious (visual inspection) or expensive (vision systems).

This paper describes a technique for electrical bond location which involves the use of a special test die. Thus conventional electrical test equipment may be used to acquire bond location data for large sample sizes. This provides a tool for studies aimed at reducing the positional variability of the bonding process. An outcome might be, for example, an opportunity to reduce the size and pitch of bond pads.

The Bond Position Sense Test Die

It is useful to have a test die which can be made to fit any package. This can be accomplished by patterning the wafer with many small dice, which we shall call "modules", and then cutting the wafer in multiples of this module to produce a die for the particular package of interest. The module size is a compromise between sufficient die-size flexibility (smaller gives more flexibility), and bond pad constraints (larger permits more pads).

The metal level of the position sense test die module is shown in Fig. 1. These modules are patterned on the wafer in a square array with center-to-center spacing 62.5 mils. Each module consists of four 5-pad sensors. The corner pads are the position-sensitive pads on which the position of the bond can be measured electrically. Two masks are required to produce the test die: the metal level shown in Fig. 1, and a passivation opening mask. The passivation opening for all of the pads is larger than for normal product, and the corner pads are larger than the others. The dimensions are given in Table I. A larger position-sensitive pad means better spatial resolution.

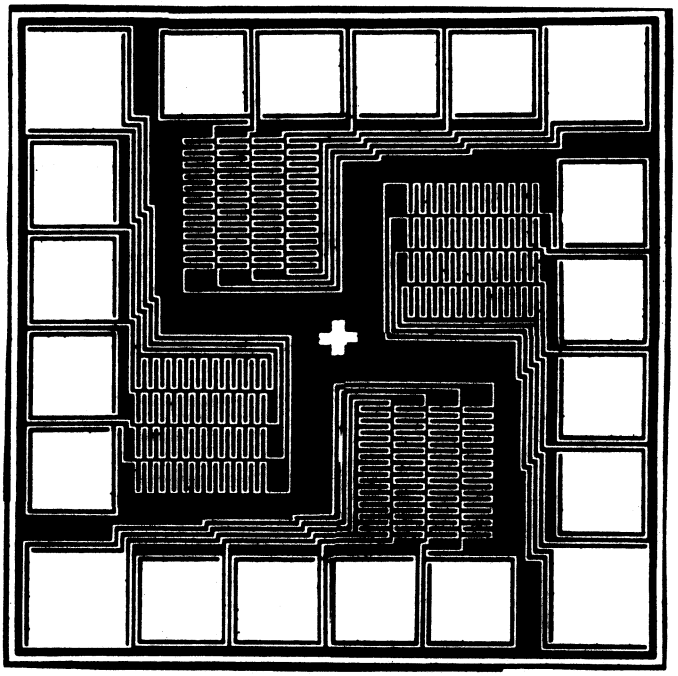

Fig. 1. Test chip module with four 5-pad sensors. The corner pads are the position-sensitive pads.

TABLE I. BOND PAD DIMENSIONS (MICRONS)[1]

	Metal Pad	Passivation Opening
Corner[2]	210	178
Edge[3]	178	122

Notes:

1. Dimensions of sides of square.
2. Position-sensitive pad.
3. Source/sense pad.

The 5-pad sensor can be used to make four kinds of measurement:

1. The corners of each position-sensitive pad are connected to four pads (source/sense pads) on an adjacent edge of the module. See Fig. 1. Each connection consists of an aluminum meander. Continuity of the meanders can be used as an indication of corrosion in moisture-related studies.

2. The test die can also be used to make Kelvin measurements of wire resistance[1]. In Fig. 2, if the current is forced into the lead finger E, through the wire W, and is withdrawn through the corner of the position-sensitive pad R and if adjacent lead fingers E and F are bonded as shown, then the potential of F relative to O, P, or Q is easily measured because O, P, and Q are connected to other lead fingers via the source/sense pads on the adjacent edge of the module. This gives the total resistance of the wire and its interfaces to pad and lead finger (typically 50 milliohms, for a normal bond). This is a four-point measurement which eliminates contributions from all of the connections to the pad OPQR and the lead finger E. It is useful as a sensitive monitor of degradation of the bond interfaces, or of wire damage.

3. Again, consider a current forced as in Fig. 2. If the current is withdrawn through the corner R via another pad (on the adjacent edge of the module) and lead finger, then a potential difference will occur between any two of the other corners (O, P, Q) of the position-sensitive pad. For a current withdrawn from R, we are particularly interested in the potential of Q relative to O. We shall define this potential as V1. No current flows into or out of the corners O and Q of the position-sensitive pad, so the potential difference between O and Q also appears on the corresponding source/sense pads on the adjacent edge of the module, and therefore also on the package pins to which these pads are bonded. Similarly, if the current is withdrawn from O, then the potential, V2, of P relative to R can be measured. The potentials V1 and V2 can be used to locate the ball bond. The magnitudes of V1 and V2 are typically equivalent to 10 milliohms or less, depending on the position of the ball bond.

4. A position-sensitive pad without a bond, but with bonds connected to its corresponding source/sense pads is a van-der Pauw element[2] which can be used to measure the sheet resistance of the aluminum. Consider a current I forced into one corner of the position sensitive pad and withdrawn through an adjacent corner. If the measured potential difference between the other corners is V, then the aluminum sheet resistance is given by

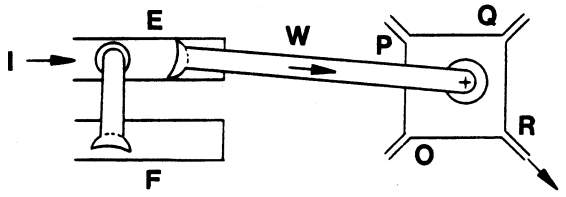

Fig. 2. Position-sensitive bond pad connected to lead finger (E) by wire. The position sensitive pad has electrical connection to other pads at its corners (O, P, Q, R). Lead finger E is jumpered to lead finger F to permit Kelvin measurement of the wire resistance.

$$\rho = \frac{\pi}{\ln 2}\,\frac{V}{I} \qquad (1)$$

Notice that measurement capabilities 2, 3, and 4 are all 4-point measurements. This means that resistance variations in the test leads (due to socketing etc.) do not affect the results.

Capabilities 3 and 4, above, of the test die were used in the study described in this paper.

Experiment

Test dice consisting of a 6x6 array (375 mils square) of the modules shown in Fig. 1 were eutectically die-attached into 68 pin laminated ceramic pin-grid array packages. Wire bonding was done according to the bonding diagram in Fig. 3. In Fig. 3 each module is represented only by its bond pads. The small arrow next to the source/sense pads indicates the position-sense pad to which they are connected. 180 units were assembled in this way.

A Keithley 350i parametric tester was used to make several of each of the four types of measurement described above for each package. We shall, however, describe only a subset of the results which illustrates the operation of the position sensor. The sheet resistance for each die was measured using pad F in Fig. 3. This was typically 0.025 ohms/square. V1 and V2 were also measured for bonds at pads A, B, C, D, and E for a forced current, I, of 100mA. The bonds at these pads were intentionally mis-positioned in various ways. The orientation convention for V1 and V2 is shown in Fig. 4. Fig. 3 and Fig. 4 have the same orientation. For example, V1 for pad A is the potential of the top right corner relative to the bottom left when the current is withdrawn from the bottom right corner.

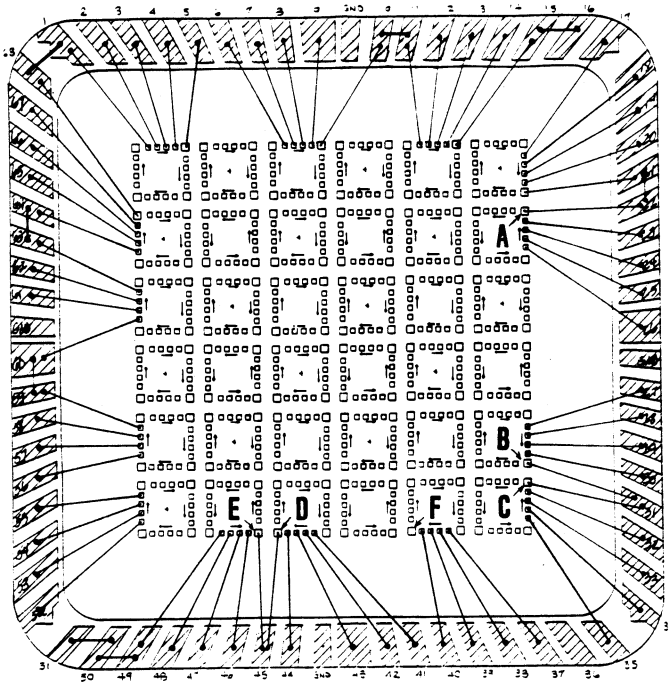

Fig. 3. Bonding diagram for 6x6 (375 mils square) test chip in a 68 pin ceramic pin-grid array package. Electrical measurements on pads A through F provided the data reported in this study. Pad F has no bond attached: it was used as a van der Pauw element to measure the sheet resistance of the aluminum.

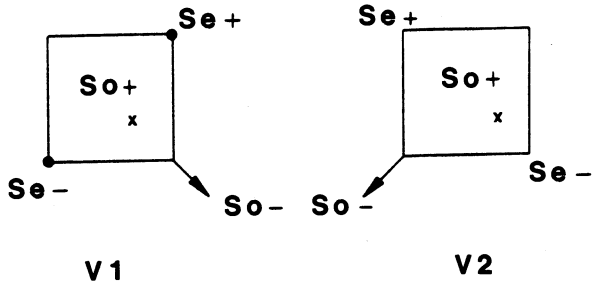

Fig. 4. Conventions defining V1 and V2. Four-terminal voltmeter connections are shown. For example, V1 is the potential of the upper right corner of the position sensitive pad relative to the lower left corner, while the current is sunk from the lower right corner. The pads in Fig. 3 and Fig. 4 have the same orientation.

For each piece the measured potentials V1 and V2 were scaled to the forced current and to the measured sheet resistance for that piece:

$$U1 = V1/\rho I \qquad (2a)$$

$$U2 = V2/\rho I. \qquad (2b)$$

The dimensionless quantities U1 and U2 are the most convenient way in which to express the results. They are independent of the film to which the bonds are made and of the measurement current chosen.

U1 and U2 for each of the 5 bonds on each of the 180 units measured are plotted in Fig. 5. The measurement error in U1 and U2, estimated by repeated measurements of the same unit (including resocketing) is less than ±0.01. Thus, in addition to the effect of the intentional mis-positioning of the bonds B, C, D, and E, the observed scatter in U1 and U2 of approximately ±0.1 is characteristic of the bonding process.

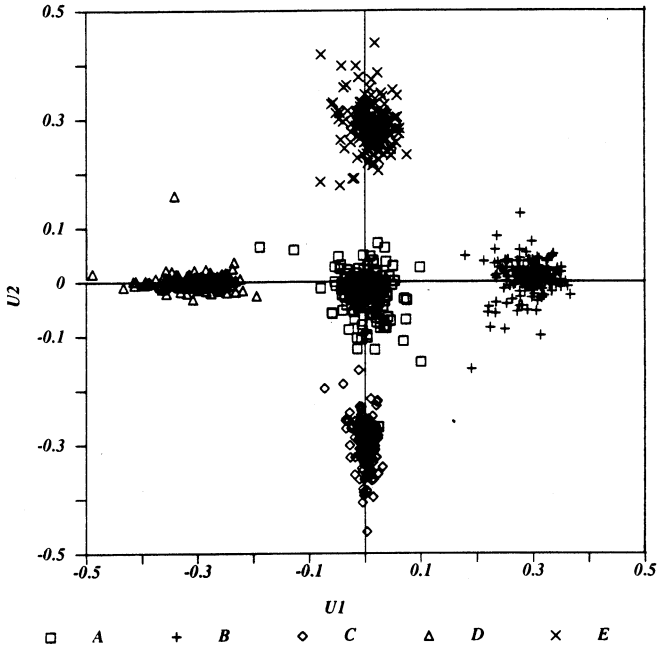

Fig. 5. Scatter plot of U1 versus U2 for each of the bonds A through F indicated in Fig. 3. Data for 180 units.

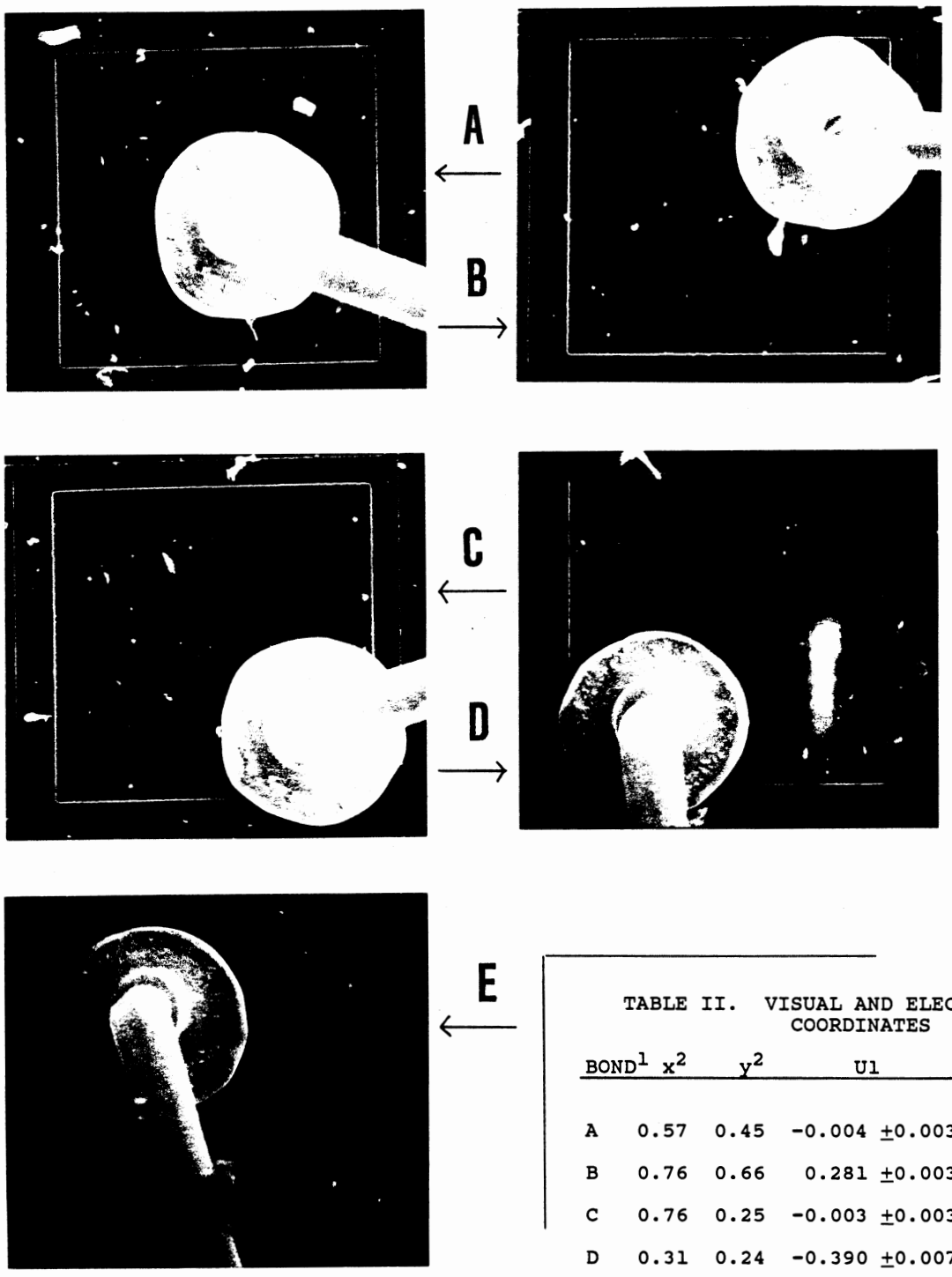

Fig. 6. Photographs of bonds A through E for the unit which provided the data in Table II.

TABLE II. VISUAL AND ELECTRICAL BOND COORDINATES

BOND[1]	x^2	y^2	U1	U2
A	0.57	0.45	-0.004 ±0.003	-0.066 ±0.004
B	0.76	0.66	0.281 ±0.003	-0.056 ±0.003
C	0.76	0.25	-0.003 ±0.003	-0.376 ±0.007
D	0.31	0.24	-0.390 ±0.007	-0.004 ±0.003
E	0.32	0.67	-0.025 ±0.004	0.238 ±0.002

Notes:

1. Bonds shown in Fig. 6.
2. Center of ball bond relative to lower-left corner of position sensitive pad, in units of pad dimensions. Eg. (0.5, 0.5) is the center of the pad.

One unit was taken for careful study. Photographs of the bonds A through E are shown in Fig. 6. The positions of the centers of the bonds relative to the lower left corner of the metal (not the passivation opening) were measured in units of the x and y dimensions of the position-sensitive pad, and the results are given in Table II. The corresponding electrically measured values of U1 and U2 are also given. The errors given for U1 and U2 correspond to repeated socketing.

Analysis

It would be useful to have a method to relate the measured values of U1 and U2 to the actual bond locations. For a finite bond size this is a complicated problem in potential theory. However, if the bond is replaced by a point source, the analysis is tractable and a reasonable approximate relationship between U1 and U2 and the location of the bond centers can be obtained. We can test the adequacy of the approximation with the data in Table II.

Consider a square conductive sheet with sides of length unity, Fig. 7. The sheet has sheet resistivity ρ. Point S, at an arbitrary location $S = x\hat{x} + y\hat{y}$ is a source of current I injected into the sheet. $\hat{x}$ and $\hat{y}$ are unit vectors in the x and y directions and $0 \leq x \leq 1$ and $0 \leq y \leq 1$ are the coordinates of S expressed as fractions of the dimensions of the sheet. The current is withdrawn at the origin of coordinates, O, and the potential difference of the corner P relative to the corner R, V2, is measured. We seek an expression for V2 as a function of the coordinates of S.

The problem of a finite sheet conductor with a source and a sink is equivalent to the problem of an infinite conducting sheet with multiple sources and sinks placed so that part of the infinite sheet has the same potential distribution as the finite sheet. The problem of the finite sheet can therefore be solved by considering the infinite sheet and summing the contributions due the multiple sources. This technique is known as the method of images. The infinite sheet equivalent to the finite sheet is also shown in Fig. 7. The point source S in the finite sheet at (x,y) has become four sources at (x,y), (-x,y), (-x,-y), (x,-y) sources a current of I (i.e. has magnitude I). The point sink at the origin, O, remains but it now sinks a current of 4I (i.e. has magnitude -4I). This pattern of four sources and a sink is repeated at each "even,even" lattice site, (0,2), (2,2), etc.

The potential of P relative to R due to a source of magnitude I_i at an arbitrary location R_i is given by elementary potential theory as:

$$V_{PR}(i) = \frac{\rho I_i}{2\pi} \ln \frac{|\hat{x} - R_i|}{|\hat{y} - R_i|} \qquad (3)$$

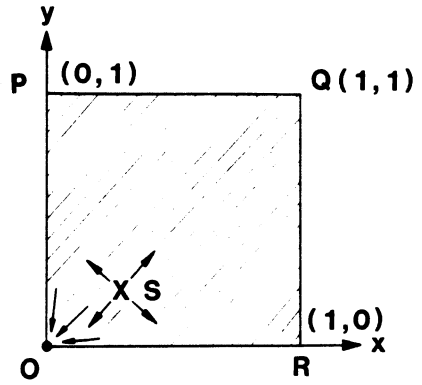

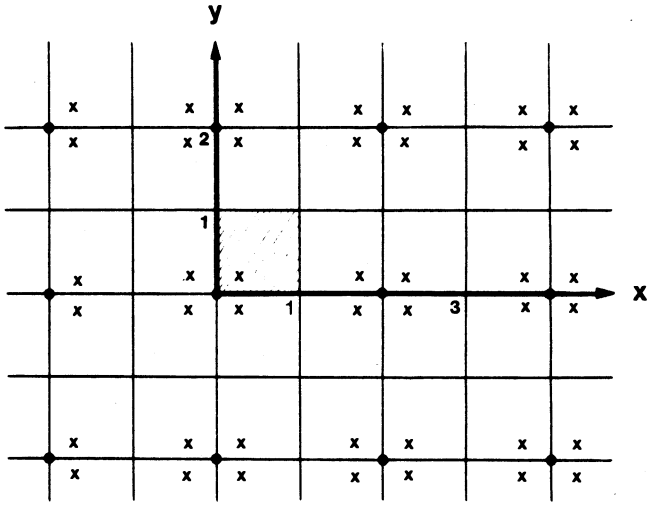

Fig. 7. Top: Finite conducting sheet with point source at S and sink at O. Bottom: Equivalent infinite conducting sheet with image sources and sinks.

The superposition principle allows one to calculate the total potential V2 by summing Eq. (3) over all sources and sinks (summing on i).

An interesting result is that the symmetry of the lattice in Fig. 7 means that the sinks have no net effect on V2. This because the effect of the sink at (m,n) (where n and m are even integers) cancels the effect of the sink at (n,m), and all sinks may be paired up in this way. Sinks at (n,n) have zero contribution to V2 since such a sink is equidistant from P and R.

Another interesting result is that the measured potential V2 is independent of whether the current is sunk at O or Q. This is because an array of sinks equivalent to Q also has no net contribution to V2. It is a result of the principle of superposition that this is true even for an extended source (such as a real bond). We have also verified this experimentally.

Thus the total effect on V2 may be calculated by summing Eq. (3) over just the sources.

$$V2 = \sum_{i(\text{Sources})} V_{PR}(i)$$

$$= \rho I \frac{1}{2\pi} \sum_{i(\text{Sources})} \ln \frac{|\hat{\underset{\sim}{X}} - \underset{\sim}{R}_i|}{|\hat{\underset{\sim}{Y}} - \underset{\sim}{R}_i|} \qquad (4)$$

$$= \rho I U2 \qquad (5)$$

where U2 is defined by

$$U2 = \frac{1}{2\pi} \sum_{i(\text{Sources})} \ln \frac{|\hat{\underset{\sim}{X}} - \underset{\sim}{R}_i|}{|\hat{\underset{\sim}{Y}} - \underset{\sim}{R}_i|} \qquad (6)$$

and where we have used the fact that each source has magnitude I. Notice that U2 in Eq. (5) has the same definition as the experimentally defined parameter in Eq. (2b). Similar expressions can be derived for U1.

We have written a computer program which generates a contour plot of U1 and U2 as a function of point source coordinates (x,y). The contour plots for U1 and U2 are superimposed in Fig. 8.

Fig. 8 allows one to translate the electrical results U1 and U2 into the actual coordinates of the current source, assuming that it is a point source. As a test of the error introduced by the fact that the bonds are actually extended sources, the electrical results (U1, U2) from Table II are plotted on the curvilinear grid (solid points), while the corresponding visually measured true positions are plotted on the x-y axes as open points. The corresponding points are connected by a bar. The point-source theory gives bond positions closer to the center of the pad than the actual positions.

Conclusions

The main disadvantage of the electrical bond position sensor is that it requires a special test die. However, once the die is available it is easy to obtain accurate positional data for large numbers of packages and many bonds within each package. This permits a statistical evaluation of bond position accuracy. This previously required expensive vision equipment or tedious inspection. All of the electrical measurements are Kelvin measurements so that socketing resistances do not affect the results.

The accuracy of the technique is very good. The measurement error of ±0.01 in U1 and U2 corresponds to a positional error of approximately ±2 microns. Intentional displacements of 60 microns, and the positional scatter of the bonding process (about ±11 microns) were easily resolved.

The positions predicted by the point source theory provides reasonable agreement with the actual observed positions. But the error in the model is greater than the sensitivity of the measurement technique. So a more realistic model would be useful. A place to start would be to extend the model to a distributed source, including the effect of occlusion by passivation when the bond overlaps it.

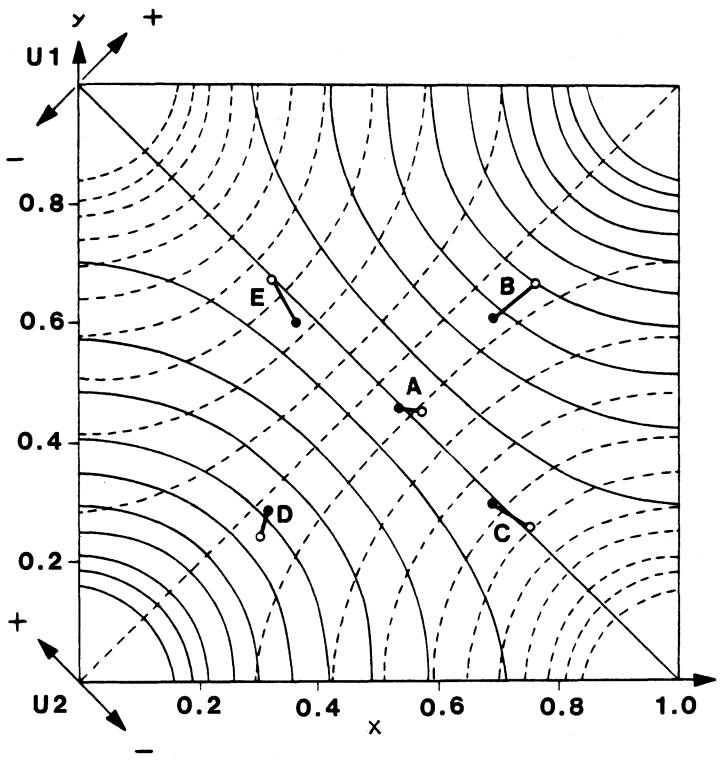

Fig. 8. Contour plot for U1 (solid lines) and U2 (broken lines) as a function of relative pad coordinates. The contour interval is 0.1. Each contour is the locus of a point source which provides a given value of U1 or U2. The location of the point sources which would give values of U1 and U2 in Table II are plotted as solid points. The measured (x,y) coordinates from Table II are plotted as open symbols.

However, application of the technique does not require an accurate model. Direct U1 vs U2 plots such as Fig. 5 provide sufficient information to optimize a bonding process.

Acknowledgements

Thanks are due to Subroto Bose, who contributed to the design of the test chip, and to Rich Blish for many useful discussions.

References

[1] R. C. Blish, II and L. Parobek, "Wire Bond Integrity Test Chip," Proc. 21st Ann. International Reliability Physics Symposium, pp142-147 (1983)

[2] L. J. van der Pauw, "A Method of Measuring Specific Resistivity and Hall Effect of Discs of Arbitrary Shape," Philips Research Reports, Vol. 13, pp1-9, (1958)